

Cite this article as: Hou Jing, Yang Peizhi, Zheng Qinrong, et al. Preparation of Magnéli Phase  $Ti_nO_{2n-1}$  by Carbothermal Reduction Sieving Method in Air Atmosphere[J]. Rare Metal Materials and Engineering, 2021, 50(11): 3824-3827.

LETTER

# Preparation of Magnéli Phase $Ti_nO_{2n-1}$ by Carbothermal Reduction Sieving Method in Air Atmosphere

Hou Jing<sup>1,2</sup>, Yang Peizhi<sup>1</sup>, Zheng Qinrong<sup>1</sup>, Wu Enhui<sup>2</sup>, Li Jun<sup>2</sup>

<sup>1</sup> Yunnan Normal University, Kunming 650500, China; <sup>2</sup> Panzhihua University, Panzhihua 617000, China

**Abstract:** A novel method for fabricating Magnéli phase (MP)  $Ti_nO_{2n-1}$  ( $4 < n < 10$ ), carbothermal reduction sieving, in air atmosphere was introduced. The influence of the reduction temperature and reduction time on the phase structure and resistivity of reduction product was investigated. The results show that increasing the reduction temperature and prolonging the reduction time are beneficial for the reduction of  $TiO_2$  to MP  $Ti_nO_{2n-1}$ . MP  $Ti_nO_{2n-1}$  ( $n=4, 5$ ) powder was obtained after reduction at 1350 °C for 20 min, and its particle size is 0.5–8 μm according to results of scanning electron microscopy analysis. Resistivity of the reduction product is decreased significantly with prolonging the reduction time at 1350 °C. The minimum resistivity of 79.3 Ω·cm is achieved for the product after reduction at 1350 °C for 50 min, and the phase composition is mainly  $Ti_3O_5$ .

**Key words:** carbothermal reduction; sieving; Magnéli phase  $Ti_nO_{2n-1}$ ; resistivity;  $TiO_2$ ; phase transformation

Nano-structured powder materials with high electro-magnetic response and energy conversion have always been a hotspot of extensive researches<sup>[1,2]</sup>. Magnéli phases (MPs) of titanium oxide, namely  $Ti_nO_{2n-1}$  ( $3 \leq n \leq 10$ ), have attracted considerable attention since 1956<sup>[3]</sup>, which possess outstanding conductivity and excellent chemical inertness, and exhibit great potential as a novel material in the fields of electrochemistry, photocatalysis, electrocatalysis, energy storage, and thermoelectricity<sup>[4-8]</sup>.  $Ti_nO_{2n-1}$  phases can be prepared by gas reduction, metal reduction, and carbothermal reduction<sup>[9-13]</sup>. Among these preparation methods, the synthesis of  $Ti_nO_{2n-1}$  by carbothermal reduction method attracts much attention owing to its advantages of relatively high reaction rate, simple procedure, high security, and low cost<sup>[14-16]</sup>. Carbothermal reduction of  $TiO_2$  can be used to prepare MP  $Ti_nO_{2n-1}$  powder which exhibits relatively high conductivity and good corrosion resistance in acidic solution. Besides, the absorption bands of MP  $Ti_nO_{2n-1}$  powder cover the full visible-light region<sup>[17,18]</sup>. However, in order to ensure that the reduction products are not oxidized, the preparation of MP  $Ti_nO_{2n-1}$  by carbothermal reduction must be conducted in either a vacuum or an inert and reducing gas atmosphere<sup>[19-23]</sup>. In addition, a small amount of carbon may remain in the reduction products, thereby affecting the purity of the

reduction products. In this research, MP  $Ti_nO_{2n-1}$  powder was synthesized from anatase  $TiO_2$  by carbothermal reduction sieving method in air atmosphere through the difference between the particle sizes of  $TiO_2$  and graphite. The influence of the reduction temperature and reduction time on the reduction phase was investigated, and the formation and characterization of the reduction products were identified.

## 1 Experiment

The anatase  $TiO_2$  powder was prepared into particles of 3~5 mm in size with deionized water, and the particles were dried at 120 °C for 2 h. Then the  $TiO_2$  particles were placed into a graphite crucible, and the periphery of the  $TiO_2$  particles was covered with graphite powder. Subsequently, the  $TiO_2$  particles were reduced in a box-type furnace under different reduction conditions. The mixture of graphite powder and reduced particles was then sieved using a vibrating screen. Finally, the reduced particles were washed by alcohol and then the products were crushed by milling. Fig. 1 shows the preparation process of  $Ti_nO_{2n-1}$ .

The reduction products were identified using X-ray diffraction (XRD) with Cu K $\alpha$  radiation (D8 ADVANCE, Bruker, Germany) with  $2\theta=10^\circ\sim90^\circ$ . The microstructure was studied using scanning electron microscopy (SEM, Quanta-

Received date: December 29, 2020

Foundation item: National Natural Science Foundation of China (U1802257)

Corresponding author: Hou Jing, Candidate for Ph. D., Yunnan Normal University, Kunming 650500, P. R. China, E-mail: houjing1108@163.com

Copyright © 2021, Northwest Institute for Nonferrous Metal Research. Published by Science Press. All rights reserved.

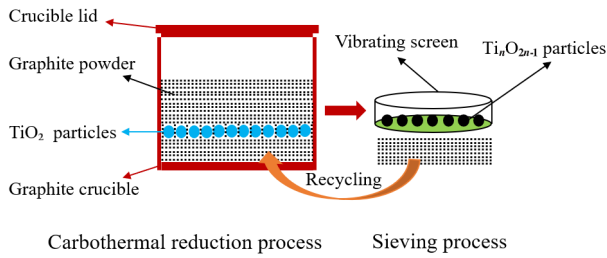


Fig.1 Schematic diagram of preparation process of  $Ti_nO_{2n-1}$

400, FEI Corporation, Netherlands) and X-ray photoelectron spectroscopy (XPS, 250XI, Thermo Electron, USA). The resistivity and density of the specimens were tested using four-probe measurements (ST2722-SZ, JG, China).

## 2 Results and Discussion

Fig. 2a shows XRD patterns of the raw material and five specimens prepared at 950~1350 °C for 20 min. The main phase of the raw material and specimen reduced at 950 °C is clearly the anatase  $TiO_2$  phase, whereas the rutile  $TiO_2$  phase appears in the specimen reduced at 1050 °C. This phenomenon indicates that the phase-transformation temperature of  $TiO_2$  is 950~1050 °C. The phase of the specimens reduced at 1050~1250 °C still contains rutile phase  $TiO_2$ , but the peak shape is gradually broadened with increasing the reduction temperature. When the reduction temperature reaches 1350 °C, the component is transformed into a mixture of  $Ti_5O_9$ ,  $Ti_4O_7$ , and  $TiO_2$  (rutile). These results show that the reduction extent of titanium dioxide is increased with increasing the temperature from 950 °C to 1350 °C. Therefore, the proper reduction temperature for synthesizing  $Ti_nO_{2n-1}$  is about 1350 °C

when reduction time is set as 20 min.

Fig. 2b shows the XRD patterns of specimens prepared by reducing anatase  $TiO_2$  in air at 1350 °C for 5~50 min. The phase in specimens reduced for 5~10 min is mainly rutile  $TiO_2$ , and the phase-transformation time of  $TiO_2$  at 1350 °C is less than 5 min. With further reducing the specimens,  $Ti_5O_9$  appears after reduction for 15 min, and the phases become  $Ti_5O_9$  and  $Ti_4O_7$  when the reduction time increases to 20 min. After reduction for 30 min, the  $Ti_3O_5$  phase appears while the peak intensities of  $TiO_2$ ,  $Ti_4O_7$ , and  $Ti_5O_9$  phases decrease. After reduction for 50 min, the specimens are reduced almost exclusively to  $Ti_3O_5$ , and  $Ti_4O_7$  and  $Ti_5O_9$  phases disappear. These results indicate that when carbothermal reduction in air at 1350 °C proceeds from 0 min to 50 min, the  $TiO_2$  (anatase),  $TiO_2$  (rutile),  $Ti_5O_9$ ,  $Ti_3O_5$ ,  $Ti_4O_7$ , and  $Ti_3O_5$  phases appear orderly.

To investigate the change mechanism of surface components during carbothermal reduction, Ti 2p peaks of the raw material and specimens reduced at 1350 °C for 20 min were obtained by XPS analysis (Fig. 3). For the raw material anatase  $TiO_2$ , the binding energy of Ti 2p exhibits a sharp peak without shoulder peak. The peaks around 458.47 and 464.17 eV can be regarded as the  $Ti^{4+} 2p_{3/2}$  and  $Ti^{4+} 2p_{1/2}$ , respectively, as shown in Fig. 3a. The binding energies of  $Ti^{4+} 2p_{3/2}$  and  $Ti^{4+} 2p_{1/2}$  are consistent with those of pure anatase  $TiO_2$  (458.4 and 464.2 eV)<sup>[23]</sup>. After carbothermal reduction, the peaks observed at 458.58 and 464.28 eV correspond to  $Ti^{4+} 2p_{3/2}$  and  $Ti^{4+} 2p_{1/2}$ , respectively, as shown in Fig. 3b, which are both in agreement with the data of rutile  $TiO_2$ <sup>[19]</sup>. Meanwhile, the tails located at 456.86 and 460.86 eV can be attributed to the existence of  $Ti^{3+}$  in  $Ti_2O_3$ . The valence states of Ti in  $Ti_nO_{2n-1}$  are consistent with those reported by Takimoto et al<sup>[24]</sup>.

Fig. 4 shows SEM morphologies of anatase  $TiO_2$  material

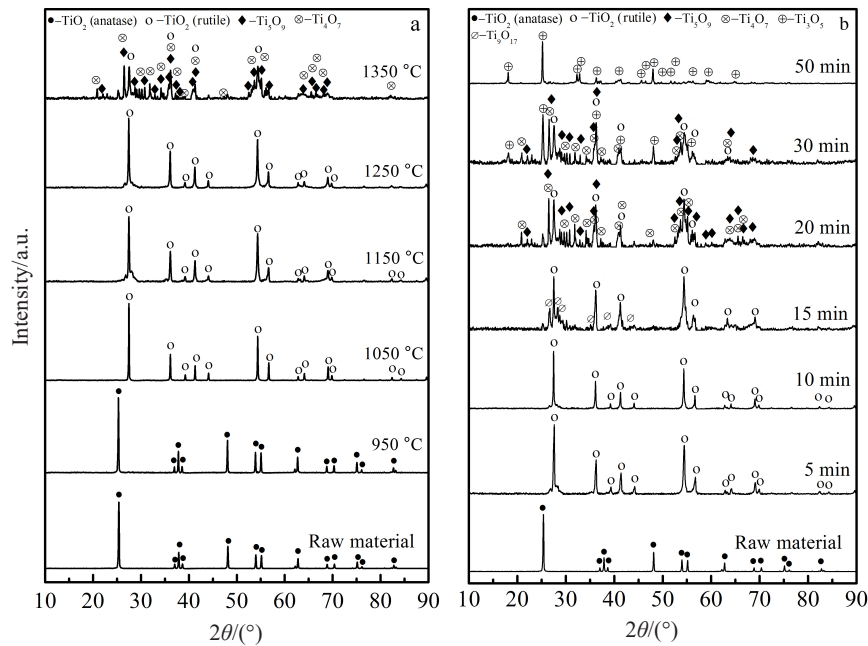


Fig.2 XRD patterns of raw material and specimens reduced at different temperatures for 20 min (a) and at 1350 °C for different durations (b)

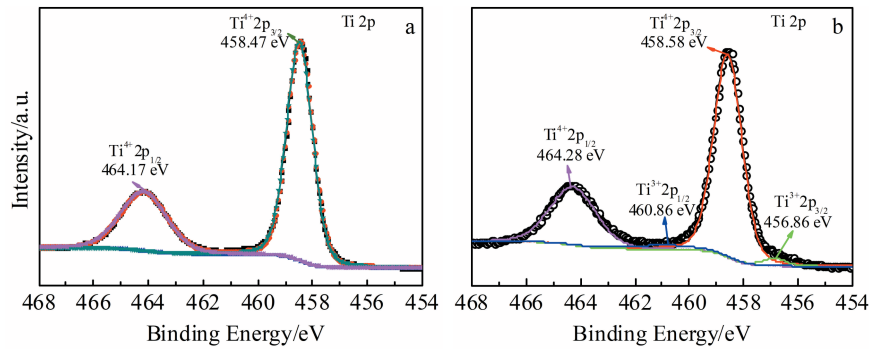


Fig.3 XPS spectra of Ti 2p of raw material anatase TiO<sub>2</sub> (a) and specimen reduced at 1350 °C for 20 min (b)

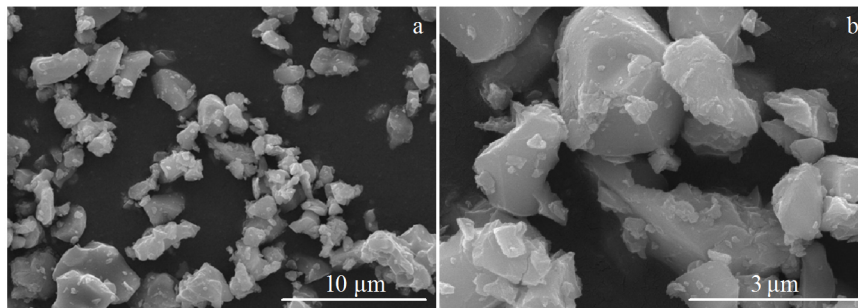


Fig.4 SEM morphologies of specimen reduced at 1350 °C for 20 min at low (a) and high (b) magnification

reduced at 1350 °C for 20 min. Fig.4a shows that the particles are irregularly shaped and distributed homogeneously, whereas Fig.4b shows clearly that there are a small number of large particles with many small pores on the surfaces and large particle gap. In addition, a loose structure is formed by CO gas escaping easily to the atmosphere, and the particle sizes are 0.5~8 μm.

The powder was compacted by a uniaxial press under a pressure of 18 MPa into a cylinder for resistivity and density measurement. The resistivity and density of different specimens are listed in Table 1. The density is decreased slightly with prolonging the reduction time, whereas the resistivity is decreased significantly. Compared with the results in Ref.[25], the resistivity of the reduced specimens is much higher because of the existence of a certain amount of TiO<sub>2</sub> (rutile) in the specimens. The specimen reduced for 50 min shows the lowest resistivity of 79.3 Ω·cm because the phase component is mainly Ti<sub>3</sub>O<sub>5</sub>.

Fig. 5 shows transmission electron microscope (TEM) images of MP Ti<sub>n</sub>O<sub>2n-1</sub> reduced at 1350 °C for 50 min. The

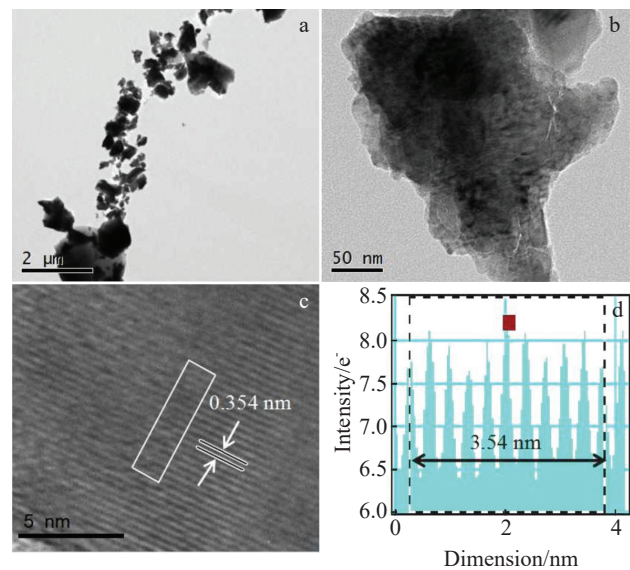


Fig.5 TEM (a, b) and high resolution TEM (c) images of MP Ti<sub>n</sub>O<sub>2n-1</sub> reduced at 1350 °C for 50 min; interplanar spacing analysis (d)

Table 1 Density and resistivity of specimens reduced at 1350 °C for different time

Reduction time/min	Density/g·cm <sup>-3</sup>	Resistivity/Ω·cm	Phase component
20	2.59	64 700	TiO <sub>2</sub> (rutile)+Ti <sub>5</sub> O <sub>9</sub> +Ti <sub>4</sub> O <sub>7</sub>
30	2.51	2245	TiO <sub>2</sub> (rutile)+Ti <sub>5</sub> O <sub>9</sub> +Ti <sub>4</sub> O <sub>7</sub> +Ti <sub>3</sub> O <sub>5</sub>
50	2.50	79.3	Ti <sub>3</sub> O <sub>5</sub>

crystallite with an interplanar spacing of about 0.354 nm is consistent with the distance of (110) crystalline plane of the Ti<sub>3</sub>O<sub>5</sub>, and the interplanar crystallite appears to be surrounded by amorphous layers. To investigate the light absorption of the prepared MP Ti<sub>n</sub>O<sub>2n-1</sub>, the absorption spectrum of the specimens was obtained by ultraviolet visible (UV-vis) diffuse

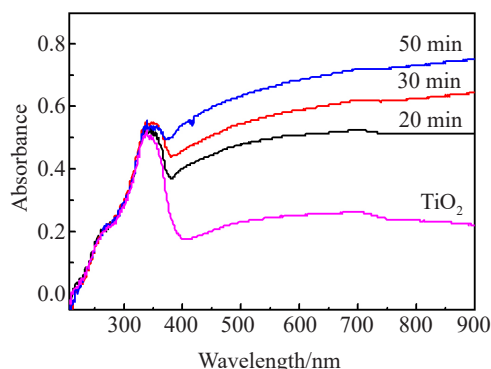


Fig.6 Absorption spectra of MP  $Ti_nO_{2n-1}$  specimens reduced at 1350 °C for different durations

reflectance spectrum from 200 nm to 900 nm at room temperature, as shown in Fig. 6. The light absorption performance is enhanced with increasing the reduction time.

### 3 Conclusions

1) Powders of Magnéli phase (MP)  $Ti_nO_{2n-1}$  ( $4 < n < 10$ ) were prepared by carbothermal reduction sieving method in air atmosphere. With prolonging the reduction time at 1350 °C, the phase of  $TiO_2$  (anatase),  $TiO_2$  (rutile),  $Ti_9O_{17}$ ,  $Ti_5O_9$ ,  $Ti_4O_7$ , and  $Ti_3O_5$  appears orderly.

2) The MP  $Ti_nO_{2n-1}$  powder exhibits low conductivity at room temperature because of the existence of a certain amount of  $TiO_2$  (rutile) in the powders. The minimum resistivity of 79.3  $\Omega \cdot cm$  is achieved after the MP  $Ti_nO_{2n-1}$  powder is reduced at 1350 °C for 50 min.

### References

- 1 Wang Xixi, Cao Wenqiang, Cao Maosheng et al. *Advanced Materials*[J], 2020, 32(36): 2 002 112
- 2 Cao Maosheng, Wang Xixi, Zhang Min et al. *Advanced Functional Materials*[J], 2019, 29(25): 1 807 398
- 3 Andersson S, Magnéli A. *Naturwissenschaften*[J], 1956, 43(21): 495
- 4 Huang Guosheng, Liu Feng, Li Xiangbo et al. *Rare Metal Materials and Engineering*[J], 2018, 47(7): 2067 (in Chinese)

- 5 Tan Jing, Mao Jian, Zhang Zhengquan. *Rare Metal Materials and Engineering*[J], 2020, 49(6): 1834
- 6 Ibrahim K B, Su W N, Tsai M C et al. *Nano Energy*[J], 2018, 47: 309
- 7 Yang Feng, Li Fan, Wang Yan et al. *Journal of Molecular Catalysis A: Chemical*[J], 2015, 400: 7
- 8 Zubair U, Amici J, Francia C et al. *ChemSusChem*[J], 2018, 11(11): 1838
- 9 Li Heping, Zhou Ting, Hu Sanyuan et al. *Chemical Engineering Journal*[J], 2017, 312: 328
- 10 Kitada A, Hasegawa G, Kobayashi Y et al. *Journal of the American Chemical Society*[J], 2012, 134(26): 10 894
- 11 Ioroi T, Siroma Z, Fujiwara N et al. *Electrochemistry Communications*[J], 2005, 7(2): 183
- 12 Li Jun, Wu Enhui, Hou Jing et al. *Rare Metal Materials and Engineering*[J], 2020, 49(7): 2281
- 13 Zhu Ruijie, Liu Ying, Ye Jinwen et al. *Journal of Materials Science Materials in Electronics*[J], 2013, 24(12): 4853
- 14 Wang Guangrui, Liu Ying, Ye Jinwen et al. *Journal of Alloys and Compounds*[J], 2017, 704: 18
- 15 Smith J R, Walsh F C, Clarke R L. *Journal of Applied Electrochemistry*[J], 1998, 28(10): 1021
- 16 Tsumura T, Hattori Y, Kaneko K et al. *Desalination*[J], 2004, 169(3): 269
- 17 Qian Shuang, Mao Jian. *Journal of Materials Science*[J], 2015, 26(7): 5166
- 18 Portehault D, Maneeratana V, Candolfi C et al. *ACS Nano*[J], 2011, 5(11): 9052
- 19 Tang Chao, Zhou Debi, Zhang Qing. *Materials Letters*[J], 2012, 79: 42
- 20 Arif A F, Balgis R, Ogi T et al. *Scientific Reports*[J], 2017, 7(1): 3646
- 21 Hao L, Kikuchi Y, Yoshida H et al. *Journal of Alloys and Compounds*[J], 2017, 722: 846
- 22 Takeuchi T, Fukushima J, Hayashi Y et al. *Catalysts*[J], 2017, 7(2): 65
- 23 Lei Yimin, Lin Xin, Hu Qihang et al. *Advanced Materials Interfaces*[J], 2018, 5(23): 1 801 256
- 24 Takimoto D, Toda Y, Tominaka S et al. *Inorganic Chemistry*[J], 2019, 58(10): 7062
- 25 Li Jun, Lu Xionggang, Yang Shaoli et al. *Chinese Journal of Rare Metals*[J], 2018, 42(6): 70 (in Chinese)

## 空气气氛下碳热还原筛分法制备 Magnéli 相 $Ti_nO_{2n-1}$

侯 静<sup>1,2</sup>, 杨培志<sup>1</sup>, 郑勤红<sup>1</sup>, 吴恩辉<sup>2</sup>, 李 军<sup>2</sup>

(1. 云南师范大学, 云南 昆明 650500)

(2. 攀枝花学院, 四川 攀枝花 617000)

**摘 要:** 介绍了一种在空气气氛中通过碳热还原筛分法制备 Magnéli 相 ( $Ti_nO_{2n-1}$ ,  $4 < n < 10$ ) 低价钛氧化物的方法, 研究了还原温度和还原时间对还原产物的物相、电阻率的影响。结果表明, 提高还原温度和延长还原时间有利于将  $TiO_2$  还原为 Magnéli 相  $Ti_nO_{2n-1}$ 。将 Magnéli 相  $Ti_nO_{2n-1}$  ( $n=4, 5$ ) 粉末在 1350 °C 下干燥 20 min, 通过扫描电子显微镜观察, 其粒径为 0.5~8  $\mu m$ 。在还原温度为 1350 °C 时, 还原产物的电阻率随还原时间的延长而显著降低。在 1350 °C 下还原 50 min 的产物的电阻率最小, 为 79.3  $\Omega \cdot cm$ , 其物相组成几乎全部为  $Ti_3O_5$ 。

**关键词:** 碳热还原; 筛分; Magnéli 相  $Ti_nO_{2n-1}$ ; 电阻率;  $TiO_2$ ; 相变

作者简介: 侯 静, 男, 1987年生, 博士生, 云南师范大学, 云南 昆明 650500, E-mail: houjing1108@163.com